

## ORIGINAL ARTICLE

Toshihiko Sunami · Kazuto Nishio  
Fumihiko Kanzawa · Kazuya Fukuoka  
Shinzo Kudoh · Jyunichi Yoshikawa · Nagahiro Saijo

## Combination effects of TAS-103, a novel dual topoisomerase I and II inhibitor, with other anticancer agents on human small cell lung cancer cells

Received: 23 March 1998 / Accepted: 15 September 1998

**Abstract Purpose:** TAS-103 [6-((2-(dimethylamino)ethyl)amino)-3-hydroxy-7H-indeno(2,1-c)quinolin-7-one dihydrochloride] is a newly synthesized dual inhibitor of topoisomerase I and II. Since anticancer drugs are used in combination with other drugs for effective chemotherapy, we investigated the cytotoxic effect of TAS-103 in combination with other conventional anticancer agents, such as cisplatin, vindesine, doxorubicin, 5-fluorouracil, and the antitopoisomerase inhibitors SN-38 and etoposide in vitro. **Methods:** Inhibition of the growth of the human small-cell lung cancer cell line SBC-3 was evaluated using the tetrazolium dye (MTT) assay. Drug interactions were evaluated by isobologram analysis and the determination of combination indices supplemented by a three-dimensional model. **Results:** Simultaneous use of TAS-103 and cisplatin had a supra-additive effect, but combinations of TAS-103 with other drugs had an additive or marginally subadditive effect. Three-dimensional model analysis added more information about the synergistic concentration ranges of two drugs (cisplatin 200–400 nM and TAS-103 7–10 nM). Sequential use of TAS-103 and cisplatin had only an additive effect. **Conclusion:** These results suggest that the concomitant use of TAS-103 and cisplatin has a greater cytotoxic effect on cancer cells than single drug use, and may provide a beneficial effect in the treatment of small-cell lung cancer.

**Key words** Novel anticancer agent · Three-dimensional method · Synergism · Combination effect · Topoisomerase inhibitor

**Abbreviations** *MTT* tetrazolium dye, *IC<sub>50</sub>* drug concentration that inhibits cell growth by 50%, *CDDP* cis-diamminedichloroplatinum(II), *VDS* vindesine, *DOX* doxorubicin, *VP-16* etoposide, *5-FU* 5-fluorouracil, *CPT-11* 7-ethyl-10-[4-(1-piperidyl)-1-piperidyl]carbonyloxy-camptothecin, *SN-38* 7-ethyl-10-hydroxy-camptothecin, *FBS* fetal bovine serum *CI* combination index, *ICL* interstrand crosslink, *TA* theoretical activity

### Introduction

DNA topoisomerases are enzymes that alter the topology of DNA by transiently breaking one or both of its strands, passing a single- or double-strand-DNA through the break, and finally rejoining the breaks. These enzymes are involved in a number of critical cellular processes, including replication, transcription, and recombination [10]. They are viewed as important targets for cancer chemotherapy, especially since it has been demonstrated that the topoisomerase I inhibitor, irinotecan chloride (CPT-11), a semisynthetic derivative of camptothecin, shows strong antitumor activity against leukemia, lymphoma [7], small-cell lung cancer [9], non-small-cell lung cancer [24], and colorectal [1], ovarian and cervical (2) cancers. The topoisomerase II inhibitor etoposide (VP-16) is also a potent anticancer agent, and combined use of VP-16 and cisplatin (CDDP) now constitutes one of the major regimens in small-cell lung cancer chemotherapy [4, 15]. It is therefore probable that topoisomerase inhibitors are promising anticancer agents.

Such an inhibitor is the novel anticancer agent 6-[[2-(dimethylamino)ethyl]amino]-3-hydroxy-7H-indeno[2,1-c]quinolin-7-one dihydrochloride (TAS-103) [26]. Its primary targets are thought to be topoisomerase I and II,

T. Sunami · K. Nishio (✉) · F. Kanzawa  
K. Fukuoka · N. Saijo  
Pharmacology Division,  
National Cancer Center Research Institute,  
1-1, Tsurumi 5-chome, Chuo-ku, Tokyo 104, Japan  
e-mail: knishio@gan2.ncc.go.jp  
Tel.: +81-(0)3-3542-2511; Fax: +81-(0)3-3542-1886

S. Kudoh · J. Yoshikawa  
First Department, Internal Medicine,  
Osaka City University, 5-7, Asahimachi 1-chome,  
Abeno-ku, Osaka 545, Japan

and its mechanism of action is believed to be stabilization of a covalent complex with DNA topoisomerase I and II. The  $IC_{50}$  of TAS-103 for topoisomerase I is said to be  $2 \mu M$ , and the  $IC_{50}$  for topoisomerase II has been determined to be  $6.5 \mu M$  in vitro [11, 20]. TAS-103 has been found to exhibit powerful and broad antitumor activity against 12 of 13 subcutaneously implanted human solid tumor xenografts including cancer of the lung, colon, stomach, breast, pancreas, and kidney [20]. However, TAS-103 has topoisomerase I inhibitor activity similar to that of SN-38, and stronger topoisomerase II inhibitory activity than VP-16 [27], and does not show any cross-resistance in several resistant phenotypes such as CDDP resistance, multidrug resistance, or topoisomerase inhibitor resistance [11]. Since anticancer drugs are used in combination with other drugs for effective chemotherapy, we investigated the cytotoxic effect of TAS-103 in combination with other established anticancer agents in vitro.

## Materials and methods

### Cell line and culture

The human small-cell lung cancer cell line SBC-3, originally established at the Okayama University School of Medicine, was donated by the Japanese Cancer Research Resources Cell Bank. The SBC-3 cells were grown as attached cultures in RPMI-1640 medium (GIBCO Co., Grand Island, N.Y.) supplemented with 10% v/v heat-inactivated fetal bovine serum (FBS; Sigma Chemical Co., St. Louis, Mo.), penicillin (100 units/ml), and streptomycin (100  $\mu g$ /ml) in a highly humidified atmosphere of 5% v/v  $CO_2$  in air at  $37^\circ C$ , as described previously. The cells were harvested routinely by mechanical disaggregation and diluted with medium to the appropriate concentrations. Cell size and numbers were determined with a Coulter Cannalyzer C-256 system (Coulter Electronics, Hialeah, Fl.).

### Drugs and chemicals

TAS-103 was provided by Taiho Chemicals Co. (Tokyo, Japan), and CDDP was purchased from Nippon Kayaku Co. (Tokyo, Japan). Paclitaxel, formulated in Cremophor EL (polyethylene glycol 35 castor oil; Parsippany, N.J.) was obtained from Bristol Myers Squibb Co. (Tokyo, Japan), vindesine (VDS) from Shionogi Co. (Osaka, Japan), VP-16 from Sigma-Aldrich Japan Co. (Tokyo, Japan) and doxorubicin (DOX) from Kyowa-Hakko-Kogyo Co. (Tokyo, Japan). SN-38 was provided by Daiichi Co. (Tokyo, Japan) and a stock solution of SN-38 was prepared in dimethylsulfoxide. Finally, 5-fluorouracil (5-FU) was provided by Mitsui Pharmaceuticals. These stock solutions and chemicals were stored at  $-20^\circ C$ .

### Growth inhibition assay

We used the tetrazolium dye (MTT) assay to evaluate the growth inhibitory effects of the drugs, as described previously [8, 18], and designed a two-way exposure schedule: concomitant exposure to two drugs for 96 h, and sequential exposure to the same drugs for 48 h each. For the concurrent schedule,  $100 \mu l$  of an exponentially growing cell suspension ( $2.5 \times 10^4$  cells/ml) was seeded into each well of a 96-well microtiter plate, then  $50 \mu l$  of TAS-103,  $50 \mu l$  of the other drug solution, and nine more steps of 1.5-fold dilution with medium were added to each well. Following exposure to the

drugs for 96 h,  $20 \mu l$  of the MTT solution [5 mg/ml in phosphate-buffered saline (PBS)] was added to each well, and the plates were incubated at  $37^\circ C$  for another 4 h. After centrifuging the plates at 200 g for 5 min, the medium was aspirated from each well as completely as possible. Next,  $200 \mu l$  of dimethylsulfoxide was added to each well to dissolve the formazan, and the optical density (absorbance) was measured at 562 and 630 nm using a Delta Soft ELISA analysis program run on a Macintosh computer interfaced with a Bio-Tek Microplate Reader (EL-340, Bio-Metallics, Princeton, N.J.).

For the sequential schedule,  $100 \mu l$  of an exponentially growing cell suspension ( $2.5 \times 10^4$  cells/ml) was seeded into each well of a 96-well microtiter plate, then  $100 \mu l$  of the first drug solution was added to each well at nine concentrations. After incubation for 48 h, the solution containing the first drug was aspirated from each well as completely as possible,  $100 \mu l$  of the second drug solution was added, and the plates were incubated at  $37^\circ C$ . Following exposure to the second drug for 48 h,  $20 \mu l$  of the MTT solution was added to each well, and absorbance was measured at 562 and 630 nm, as described above. The absorbance of wells containing only RPMI-FBS and MTT were also read as an assay control. Each experiment was performed using six replicate wells for each drug concentration. At least three independent experiments were carried out, and the  $IC_{50}$  was defined as the concentration needed for a 50% reduction of the absorbance in each test, and the surviving fraction was calculated as: (mean absorbance of six replicate wells containing drugs – mean absorbance of six replicate assay control wells)/(mean absorbance of six replicate drug-free wells – mean absorbance of six replicate assay control wells).

### Analysis of combined effects

We analyzed the effects of drug combinations using two-dimensional methods the isobologram method of Steel and Peckham [22] and the combination index (CI) method of Chou and Talalay [3]. If the combination was found to be supraadditive, it was further evaluated by a three-dimensional method.

### Combination index

This method is based on the principle that the growth inhibition curve can be represented by the median-effect equation as follows [3]:

$$f_a/f_u = (D/D_m)^m \quad (1)$$

where  $D$  is the dose administered,  $D_m$  is the dose required for 50% growth inhibition,  $f_a$  is the fraction affected by dose  $D$ ,  $f_u$  is the unaffected fraction, and 'm' is a coefficient denoting the sigmoidicity of the dose-effect curve. Theoretically, the CI is the ratio of the combined dose to the sum of the two single-agent doses at the isoeffective level. Consequently, CI values smaller than, equal to, or greater than 1 represent synergism, additivity, and antagonism, respectively.

### Isobologram

The isobologram was proposed by Loewe and Muischnek in 1926 [17], and the "envelope of additivity" was developed and introduced into isobologram analysis by Steel and Peckham [21, 22]. This method is well known and has often been used in recent studies to evaluate synergism or antagonism. If two drugs do not interact, the equation is:

$$(D)_A/(D_X)_A + (D)_B/(D_X)_B = 1 \quad (2)$$

In practice, the concentrations  $(D_X)_A$ ,  $(D_X)_B$ ,  $(D_X)_{A,B}$ , for each of two drugs and the two drugs combined, respectively, required to produce the same percentage growth inhibition, are obtained from their dose-response curves. The concentrations of drugs A and B are placed on the X and Y coordinates of the isobologram,

respectively. Three isoeffect curves (mode I, mode IIA, and mode IIB) are drawn [19]. The total area enclosed by these three lines represents the “envelope of additivity”. When the experimentally determined  $IC_{50}$  of the combination is plotted on the left side of the envelope, the interaction between the drugs in combination is considered supraadditive (synergistic). When the experimental data point is plotted within the envelope, the combination is considered additive, and when it falls on the right side of the envelope, but within the square produced by 0–1  $IC_{50}$  units, the combination is considered subadditive. When the point lies outside the square, both drugs are considered protective of each other.

### Three-dimensional model

The theoretical basis of this three-dimensional model has been described previously [14]. The CI Eq. 1 for mutually nonexclusive inhibitors  $f_a$  and  $f_b$ , with subscripts designating the drug or the combination used is,

$$\begin{aligned} (f_a)_{A,B}/(f_u)_{A,B} &= (f_a)_A/(f_u)_A + (f_a)_B/(f_u)_B \\ &+ \alpha(f_a)_A/(f_u)_B + (f_a)_B/(f_u)_A \end{aligned} \quad (3)$$

where  $(f_a)_A$ ,  $(f_a)_B$ , and  $(f_a)_{A,B}$  are the fractions affected by drug A, drug B, and their combination, respectively. And  $(f_u)_{A,B} = 1 - (f_a)_{A,B}$ ,  $(f_u)_A = 1 - (f_a)_A$ ,  $(f_u)_B = 1 - (f_a)_B$ . For mutually exclusive drugs,  $\alpha = 0$ ; for mutually nonexclusive drugs,  $\alpha = 1$ .

In the case of the combination of TAS-103 and CDDP,  $\alpha = 1$  was assumed, since TAS-103 is known to act by different mechanisms from CDDP.

For mutually nonexclusive drugs, where  $\alpha = 1$ ,

$$\begin{aligned} (f_a)_{A,B}/\{1 - (f_a)_{A,B}\} \\ &= (f_a)_A/\{1 - (f_a)_A\} + (f_a)_B/\{1 - (f_a)_B\} \\ &+ (f_a)_A(f_a)_B/\{1 - (f_a)_A\}\{1 - (f_a)_B\} \end{aligned} \quad (4)$$

Finding a common denominator and simplifying,

$$(f_a)_{A,B} = (f_a)_A + (f_a)_B - (f_a)_A(f_a)_B \quad (5)$$

Here,  $(f_a)_{A,B}$  is defined as theoretical additivity (TA), since Eq. 3 was designated from the TA,

$$TA = (f_a)_A + (f_a)_B - (f_a)_A(f_a)_B \quad (6)$$

Integrating with respect to concentration of  $(f_a)_A$  and  $(f_a)_B$ , the resulting calculated response surface  $\{(S_a)_{A,B}\}$  is simulated as shown in Fig. 1C:

$$\{(S_a)_{A,B}\}_{cal} = \int_{a=0}^n \int_{b=0}^m TA \quad (7)$$

Cytotoxicity data obtained from the experiments directly generated a dose-response surface, that is, an observed response surface as shown in Fig. 1A. This observed response surface,  $\{(S_a)_{A,B}\}_{obs}$ , was subsequently subtracted from the above theoretical calculated response surface,  $\{(S_a)_{A,B}\}_{cal}$ , as shown in Fig. 1B, to reveal the “combination effect surface”,  $\{(S_a)_{A,B}\}_{CE}$ , calculated from the combination of the two drugs (Fig. 1C):

$$\{(S_a)_{A,B}\}_{CE} = \{(S_a)_{A,B}\}_{cal} - \{(S_a)_{A,B}\}_{obs} \quad (8)$$

The combination effect surface reveals synergy or antagonism for the growth of cells cultured in a drug-free medium. To confirm whether synergism occurred or not, the upper and lower 95% confidence limits of the experimental data were compared with the calculated additivity. As shown in Fig. 4E, the “95% confidence limit surface”,  $\{(S_a)_{A,B}\}_{95\%C}$ , was calculated from standard deviations of the data  $\{(S_a)_{A,B}\}_{SD}$  and  $t$ -values  $\{(S_a)_{A,B}\}_t$ :

$$\{(S_a)_{A,B}\}_{95\%C} = \{(S_a)_{A,B}\}_{SD} \{(S_a)_{A,B}\}_t \quad (9)$$

The combination effect surface,  $\{(S_a)_{A,B}\}_{CE}$ , and the 95% confidence limit surface  $\{(S_a)_{A,B}\}_{95\%C}$ , then yielded “the modified confidence plot surface”,  $\{(S_a)_{A,B}\}_{MC}$ , (Fig. 4G):

**Fig. 1A–H** Three-dimensional analysis of the antitumor interaction of TAS-103 and CDDP, including the stages in the data transformation required for the synergy plots. **A** shows the empirical dose-response curve. Two matrices representing the cytotoxic effects of TAS-103 and CDDP alone were used to calculate the theoretical additive effect using the assumption of dissimilarity. The resulting calculated additive surface (**B**) was then subtracted from the empirical surface, yielding the synergy plot in surface (combination effect surface **C**) and contour form (**D**). The combination effect surface was then divided according to the upper and lower 95% confidence limits of the experimental data (**E**, and contour form **F**), yielding the modified confidence plot in surface (**G**) and contour form (**H**). The combination effect (%) in **C** and **D** represents there ‘quantities’ of the additive effects, and confidence grades in **G** and **H** can represent the ‘qualities’ of the effects. At TAS-103 and CDDP concentrations of approximately 2–10 nM and 100–600 nM, 6–8% synergism was observed with a statistical confidence of more than 95%

$$\{(S_a)_{A,B}\}_{MC} = \{(S_a)_{A,B}\}_{CE} / \{(S_a)_{A,B}\}_{95\%C} \quad (10)$$

If the upper confidence limit is lower than the calculated additivity, the observed synergy would be considered significant. Similarly, if the lower confidence limit is greater than the calculated additivity, the observed antagonism would be considered significant.

## Results

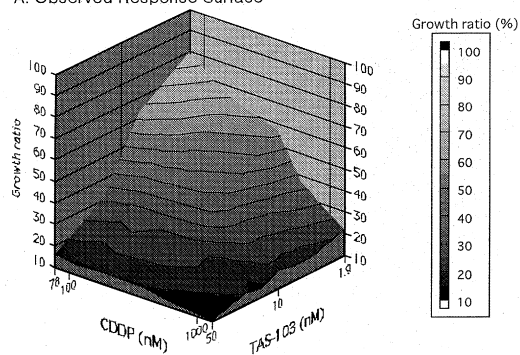
Effects of TAS-103 and other drugs, alone and in combination, on the growth of SBC-3 cells

We repeated each experiment independently at least three times. The data from the experiments were used for the different methods of analysis: the CI, isobologram analysis, and the three-dimensional model analysis. Growth inhibition curves of TAS-103 alone and in combination with other drugs against SBC-3 cells were obtained. The growth inhibition curves of TAS-103 in combination with various concentrations of CDDP (0, 78.0, 117.1, 175.6, 263.4, 395.1, 592.6, 888.9, 1333.3, and 2000 nM), and of CDDP alone and in combination with various concentrations of TAS-103 (0, 2.0, 2.9, 4.4, 6.6, 14.8, 22.2, 33.3, 50 nM), are shown in Fig. 1A and 1B, respectively. Similar dose-response curves were obtained for paclitaxel, VDS, DOX, 5-FU, SN-38, and VP-16 (data not shown). The shape of these dose-response curves is indicative of a mutually nonexclusive interaction between them. An additive effect is suggested by the difference in slope of the dose-response curves for TAS-103 at various concentrations of CDDP [3].

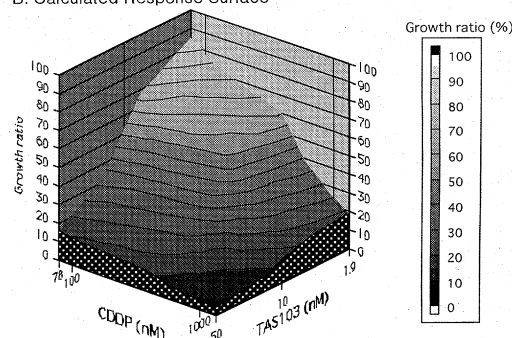
### Evaluation by combination index

We analyzed the cytotoxic interaction between TAS-103 and other drugs by the median-effect method described by Chou and Talalay [3], and evaluated the combinations in terms of synergism or antagonism. The analysis using the CI was performed for many different dose ratios, because CI values depend on drug concentrations and their molar ratios. We constructed CI plots by computer analysis, and the optimal CI values at the  $IC_{50}$  level are shown in Table 1.

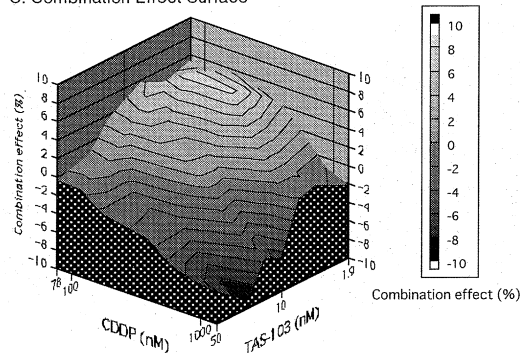
A. Observed Response Surface



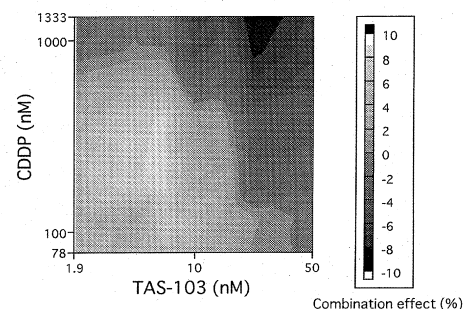
B. Calculated Response Surface



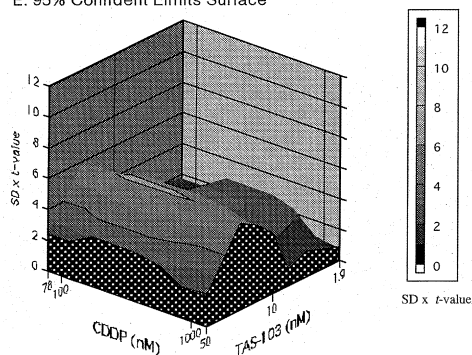
C. Combination Effect Surface



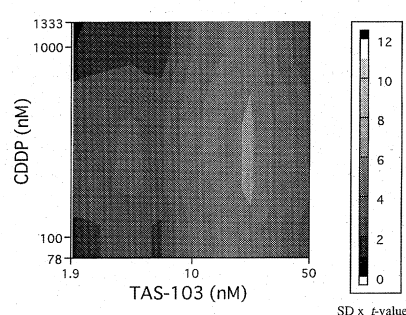
D. Contour Plot of Combination Effect Surface



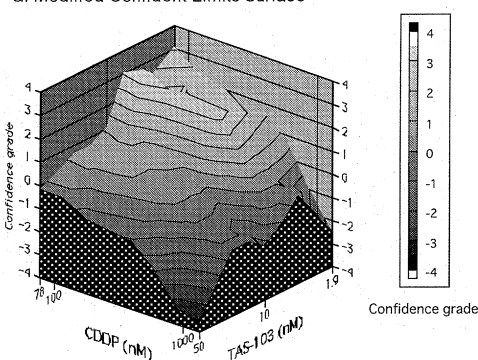
E. 95% Confident Limits Surface



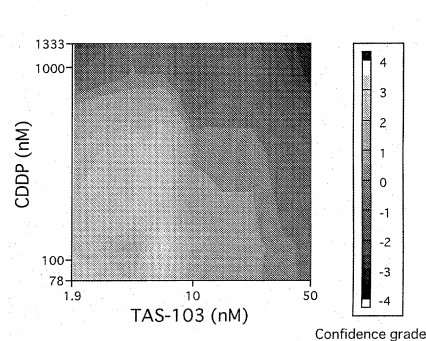
F. Contour Plot of 95% Confident Limits Surface



G. Modified Confident Limits Surface



H. Contour Plot of Modified Confident Limits Surface



A potent synergistic effect was observed only with concomitant exposure to TAS-103 and CDDP combined.

#### Evaluation by isobologram analysis

We analyzed the drug combination effects by the isobologram method of Steel and Peckham, based on the

growth inhibition curves of each drug. With this system, supraadditive, additive, and subadditive effects can be identified from the location of data points on the area of the “envelope of additivity”.  $IC_{50}$  values were calculated on the basis of growth inhibition curves of each drug, and three isoeffect curves, modes I, IIa, and IIb, were drawn. The  $IC_{50}$  drug concentrations determined from

growth inhibition curve of each drug in combination with other drugs at various concentrations were plotted on a linear scale in the isobologram.

Simultaneous and continuous exposure of SBC-3 cells to TAS-103 and CDDP (96 h) resulted in a supra-additive effect (Fig. 3A). Exposure to TAS-103 plus paclitaxel was marginally subadditive (Fig. 3B), exposure to TAS-103 plus VDS was marginally subadditive (Fig. 3C), exposure to TAS-103 plus DOX was marginally subadditive (Fig. 3D), exposure to TAS-103 plus 5-FU was additive (Fig. 3E), exposure to TAS-103 plus SN-38 was additive (Fig. 3F), and exposure to TAS-103 plus VP-16 was additive (Fig. 3G). Sequential exposure of SBC-3 cells to TAS-103 (48 h) followed by CDDP (48 h; Fig. 4A), and to CDDP followed by TAS-103 (48 h; Fig. 4B) was additive, not supraadditive. The single agent  $IC_{50}$  values for 96 h continuous treatment with CDDP, paclitaxel, VDS, DOX, 5-FU, SN-38, and VP-16 were  $330 \pm 50$ ,  $650 \pm 200$ ,  $2.3 \pm 2$ ,  $1.7 \pm 1$ ,  $650 \pm 450$ ,  $2200 \pm 1020$ ,  $1.3 \pm 0.77$ ,  $780 \pm 620$  nM (average  $\pm$  SD), respectively.

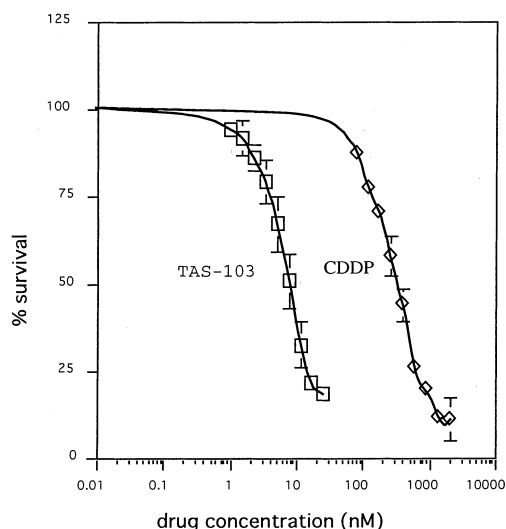
#### Evaluation by the three-dimensional model

The evaluations using the CI and isobologram methods revealed a supraadditive effect of the concomitant use of TAS-103 and CDDP, and we used the three dimensional model analysis [14] to evaluate the effects of TAS-103 and CDDP in greater detail than is possible with the conventional two-dimensional model. Figure 1 shows the three-dimensional model of the cytotoxic interaction between TAS-103 and CDDP, including the stages in the data transformation required to produce the synergy plots. The experimental dose-response curve was constructed in three dimensions (observed response surface; Fig. 1A) by using the two dose-response curves of TAS-103 and CDDP. These two curves were transformed to matrices that represented the theoretical effect of an additive combination (calculated response surface; Fig. 1B). The calculated response surface was then subtracted from the observed response surface and plotted as a three-dimensional graph and as contour forms to reveal regions of synergy or antagonism (Fig. 1C,D).

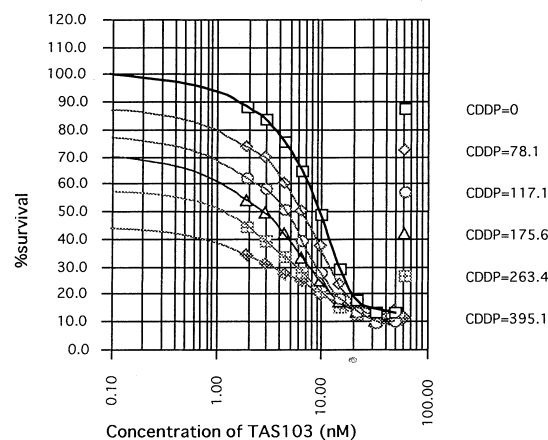
A significant synergistic region was seen in the contour plot (Fig. 1D), at TAS-103 and CDDP concentrations of approximately 2–10 nM and 100–600 nM, respectively (in the white region, the difference is over

6%). The three-dimensional graph demonstrates the concentration dependence of the drug-drug interaction and shows the complexity of the interaction between the drugs.

#### A Dose-Response Curve of TAS-103 and CDDP



#### B Dose-Response Curve of TAS103



#### C Dose-Response Curve of CDDP

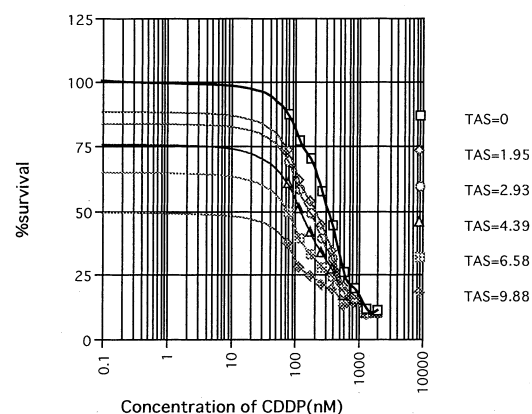


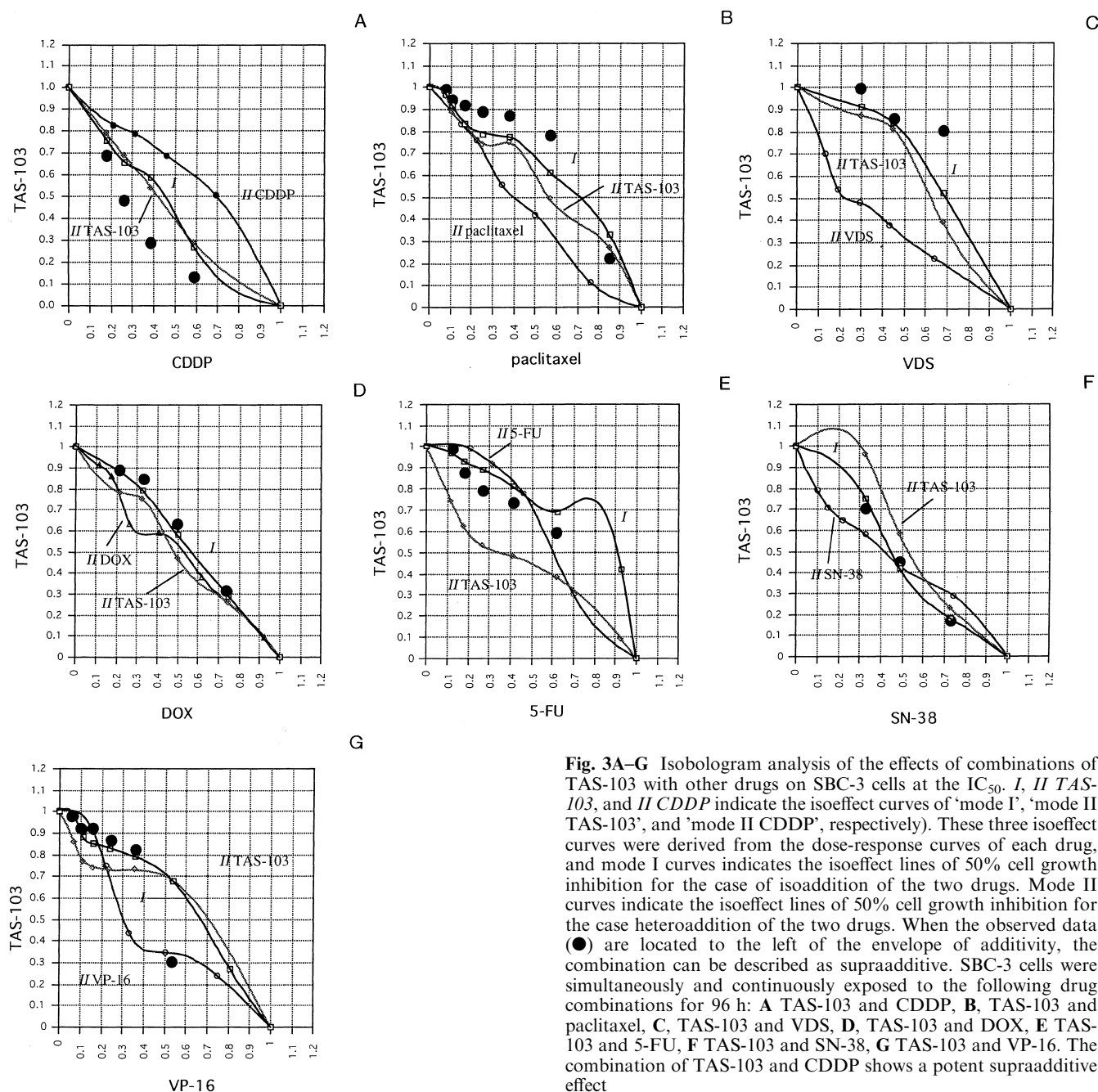
**Fig. 2A–C** Growth inhibition curves after 96 h continuous exposure to TAS-103 and CDDP of SBC-3 cells (A). Surviving fractions were evaluated using the MTT assay. The values shown are the means  $\pm$  SD from at least six independent experiments, using six replicate wells for each drug concentration. Growth inhibition curves are shown for TAS-103 in combination with various doses of CDDP (B), and for CDDP in combination with various doses of TAS-103 (C)

**Table 1** Optimal combination index (CI) values at 50% growth inhibition of SBC-3 cells by TAS-103 plus other drugs. Cells were treated with TAS-103 in combination with the other drugs at a fixed ratio. CI values <1 indicate synergism. Strong synergy is observed for CDDP

	CDDP	Paclitaxel	VDS	DOX	5-FU	SN-38	VP-16
CI at 50% fraction affected	0.501	1.237	1.341	0.970	0.869	0.934	1.091
Optimal concentration ratio of drug/TAS-103	40	1.67	4	40	40	0.4	40

To determine the significance of the differences between the observed and calculated effects, the upper and lower 95% confidence limits of the experimental data (Fig. 1E, and contour form Fig. 1F) were compared

with the calculated additive effect. The modified surface and its contour form were constructed by dividing the calculated surface and plotting as a three-dimensional graph from the 95% confidence surface (Fig. 1G,H).



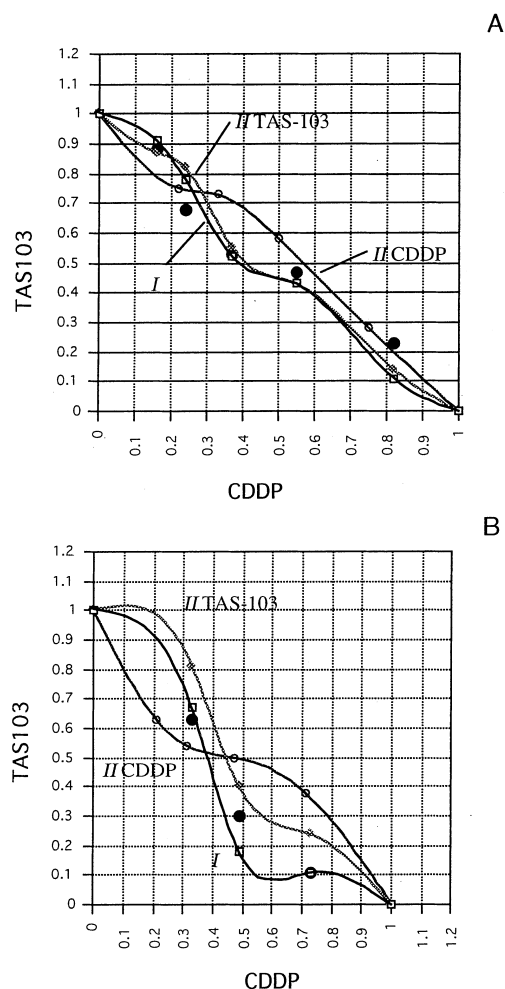


**Fig. 4A,B** Effects on SBC-3 cells of TAS-103 combined with CDDP using a sequential schedule. The drug concentrations were plotted on a linear scale relative to the  $IC_{50}$ . The SBC-3 cells were exposed to TAS-103 for 48 h followed by CDDP for 48 h (A), or exposed to CDDP for 48 h followed by TAS-103 for 48 h (B).

Since the modified surface is considered to represent statistical significance or real additive effects, the statistically reliable region of the contour plot (Fig. 1H) is at TAS-103 and CDDP concentrations of approximately 2–10 nM and 100–600 nM, respectively (within the half-tone region with confidence grades 1–4).

Thus we conclude that at TAS-103 and CDDP concentrations of approximately 2–10 nM and 100–600 nM, significant synergism occurred with enough statistical confidence.

## Discussion

TAS-103 is a newly synthesized potent inhibitor of topoisomerase I and II that acts by forming a stable covalent complex with DNA-topoisomerase I or II, as described above. DNA topoisomerase is currently one of the most important targets of antitumor agents, and indeed CPT-11 (for topoisomerase I), topotecan (for

topoisomerase II), VP-16 (for topoisomerase II) and other topoisomerase inhibitors have already been demonstrated to have strong antitumor activity against various human malignancies in clinical studies [23]. The combined use of anticancer agents is a common strategy in clinical chemotherapy, and thus the possibility of synergism and the optimal combinations of the anticancer agents should be examined. The results of our study suggest that concomitant continuous exposure to TAS-103 and CDDP has a synergistic effect on the SBC-3 cell line at concentrations of approximately 7–8 nM and 80–200 nM respectively, but that sequential use of these drugs does not result in synergism.

The combined use of CDDP and a topoisomerase inhibitor is an interesting strategy for cancer chemotherapy. A high clinical response rate has been reported for CDDP plus CPT-11 in lung cancer [5]. On the other hand, CDDP and VP-16 are active against a variety of human tumors, and this combination is considered synergistic based on the fact that therapeutic synergy has been reported in the mouse P388 *in vivo* model [20] and in human clinical trials.

At the cellular level, some studies have demonstrated a synergistic effect of CDDP combined with CPT-11 and SN-38, an active metabolite of CPT-11. Itoh et al. have observed synergistic effects of SN-38 combined with CDDP on five out of six human lung cancer cell lines [12], and Kano et al. have reported synergistic effects of CPT-11 and SN-38 combined with CDDP on acute lymphoblastic leukemia (MOLT-3) cells [13].

The interaction and biochemical mechanisms of synergy between CDDP and NB-506, a topoisomerase I inhibitor, have been examined [6]. The formation of DNA interstrand crosslinks (ICLs) in the cells was analyzed, and an increased in ICLs was observed after simultaneous exposure to CDDP and NB-506 compared with exposure to CDDP alone. DNA repair after ICL formation induced by a 3 h exposure to CDDP is also reduced by NB-506 exposure [6]. On the other hand, it has previously been reported that the biochemical mechanism responsible for the synergistic effects of CDDP and VP-16 on SBC-3 cells is enhancement of the DNA topoisomerase II inhibitory activity of VP-16 by CDDP, and the analysis *in vitro* is reflected *in vivo* [16]. The details of the biochemical mechanisms of synergy between TAS-103 and CDDP are unknown, but similar mechanisms may be applicable to topoisomerase I and II.

Isobologram analysis has shown that the effect of combined CDDP and VP-16 on human SCLC and four human NSCLC cell lines is no more than additive [19]. However, we have previously shown by three-dimensional model analysis that the combination of CDDP and VP-16 has a synergistic effect on human SCLC cell lines at concentrations of approximately 0.025–0.075  $\mu\text{g/ml}$  and 0.01–0.075  $\mu\text{g/ml}$ , respectively [14]. In the present study we were able to demonstrate a synergistic effect of TAS-103 and CDDP by three different methods of analysis, and showed that the synergistic effects depend

not only on the combination but also on the concentrations of the drugs. The three-dimensional model, as a method for evaluating the combined effect of these drugs, provided information about the optimal concentration ranges. It is very important to obtain such information before proceeding to *in vivo* studies.

Further examination of these drug interactions in preclinical studies, both *in vitro* and *in vivo*, and investigation of their mechanisms of action, would provide useful information for future combination chemotherapy regimens.

**Acknowledgement** This work was supported, in part, by Grants-in-Aid for Cancer Research, by the Second Term Comprehensive 10-Year Strategy for Cancer Control, the Ministry of Health and Welfare, and the Ministry of Education and Science in Japan. The trust fund was supported by the Taiho Pharmaceutical Co., Ltd., Tokyo, Japan under the government control.

## References

1. Aller P, Rius C, Mata F, Zorrilla A, Cabanas C, Bellon T, Bernabeu C (1992) Camptothecin induces differentiation and stimulates the expression of differentiation related genes in U-937 human promonocytic leukemia cells. *Cancer Res* 52: 1245
2. Chou S, Kaneko M, Nakaya K, Nakamura Y (1990) Induction of differentiation of human and mouse myeloid leukemia cells by camptothecin. *Biochem Biophys Res Commun* 166: 160
3. Chou TC, Talalay P (1984) Quantitative analysis of dose-effect relationships: the combined effects of multiple drugs on enzyme inhibitors. *Adv Enzyme Regul* 22: 27
4. Crino L, Tonato M, Darwish S, Meacci ML, Corgna E, Di Costanzo F, Buzzi F, Fornari G, Santi E, Ballatori E (1990) A randomized trial of three cisplatin-containing regimens in advanced non-small-cell lung cancer. *Cancer Chemother Pharmacol* 26(1): 52
5. Fujiwara Y, Yamakido M, Fukuoka M, Kudoh S, Furuse K, Ikegami H, Ariyoshi Y, for the West Japan Lung Cancer Study Group (1994) Phase II study of irinotecan (CPT-11) and cisplatin (CDDP) in patients with small cell lung cancer (SCLC). *Proc Am Soc Clin Oncol* 13: 335
6. Fukuda M, Nishio K, Kanzawa F, Ogasawara H, Ishida T, Arioka H, Bojanowski K, Oka M, Saijo N (1996) Synergism between cisplatin and topoisomerase I inhibitors, NB-506 and SN-38, in human small cell lung cancer cells. *Cancer Res* 56: 789
7. Gallo RC, Whang-Peng J, Adamson RH (1971) Studies on the antitumor activity, mechanism of action, and cell cycle effects of camptothecin. *J Natl Cancer Inst* 46: 789
8. Horiuchi N, Nakagawa K, Sasaki Y, Minato K, Fujiwara Y, Nezu K, Ohe Y, Saijo N (1988) *In vitro* antitumor activity of mitomycin C derivative (RM-49) and new anticancer antibiotics (FK973) against lung cancer cell lines determined by tetrazolium dye (MTT) assay. *Cancer Chemother Pharmacol* 22: 246
9. Horwitz SB, Horwitz MS (1973) Effects of camptothecin on the breakage and repair of DNA during the cell cycle. *Cancer Res* 33: 2834
10. Hsieh T (1990) DNA topology and its biological effects. In: Cozzarelli NR, Rang JC (eds) *DNA topology and its biological effects*. Cold Spring Harbor Laboratory Press, Cold Spring Harbor, pp 243-263
11. Ishida T, Nishio K, Arioka H, Kurosawa H, Fukumoto H, Fukuoka K, Nomoto T, Yokote H, Saijo N (1996) TAS-103, a novel dual inhibitor of DNA topoisomerase I and II. *Proc Am Assoc Cancer Res* 37: 428
12. Itoh K, Takada M, Kudo S, Masuda N, Nakagawa K, Matsui K, Takifuji N, Kusunoki Y, Fukuoka M, Kishimoto S (1991) Synergistic effects of CPT-11 and cisplatin or etoposide on human lung cancer cell lines demonstrated by computer analysis. *Lung Cancer* 7: 124
13. Kano Y, Suzuki S, Akutsu M, Suda K, Inoue Y, Yoshida M, Sakamoto S, Miura Y (1992) Effects of CPT-11 in combination with other anti-cancer agents in culture. *Int J Cancer* 50: 604
14. Kanzawa H, Nishio K, Fukuoka K, Fukuda M, Kunimoto T, Saijo N (1997) Evaluation of synergism by a novel three-dimensional model for the combined action of cisplatin and etoposide on the growth of a human small-cell lung-cancer cell line, SBC-3. *Int J Cancer* 71: 311
15. Klastersky J, Sculier JP, Lacroix H, Dabouis G, Bureau G, Libert P, Richez M, Ravez P, Vandermoten G, Thiriaux J (1990) A randomized study comparing cisplatin or carboplatin with etoposide in patients with advanced non-small-cell lung cancer: European Organization for Research and Treatment of Cancer, Protocol 07861. *J Clin Oncol* 8: 1556
16. Kondo H, Kanzawa F, Nishio K, Saito S, Saijo N (1994) *In vitro* and *in vivo* effects of cisplatin and etoposide in combination on small-cell lung-cancer cell lines. *Jpn J Cancer Res* 85: 1050
17. Loewe S, Muischnek H (1926) Über Kombinationswirkungen. I. Mitteilung: Hilfsmittel der Fragestellung. *Naunyn Schmiedebergs Arch Pharmacol* 114: 313
18. Mosmann T (1983) Rapid colorimetric assay for cellular growth and survival: application to proliferation and cytotoxic assays. *J Immunol Methods* 65: 55
19. Nakamura T, Ono M, Fukukawa M, Wada M, Kuwano M, Utsugi T, Ymada Y (1997) DNA conformational changes induced by the antitumor agent TAS-103 targeted to both topoisomerase I and II. *Proc Am Assoc Cancer Res* 38: 14
20. Schabel FM, Trader MW, Laser WR, Corbett TH, Griswold DP (1979) *cis*-Dichlorodiamineplatinum(II): combination chemotherapy and cross-resistance studies with tumors of mice. *Cancer Treat Rep* 63: 1459
21. Steel GG, Peckham MJ (1979) Exploitable mechanisms in combined radiotherapy-chemotherapy: the concept of additivity. *Int J Radiat Oncol Biol Phys* 5: 85
22. Steel GG, Peckham MJ (1979) Terminology in the description of drug-radiation interactions. *Int J Radiat Oncol Biol Phys* 5: 1145
23. Takeuchi S, Takamizawa H, Takeda Y, Ohkawa T, Tamaya T, Noda K, Sugawa T, Sekiba K, Yakushiji M, Taguchi T (1991) An early phase II study of CPT-11 in gynecologic cancers. Research Group of CPT-11 in Gynecologic Cancers (in Japanese). *Gan To Kagaku Ryoho* 18: 579
24. Tobey RA (1972) Effects of cytosine arabinoside, daunomycin, mithramycin, azacytidine, Adriamycin, and camptothecin on mammalian cell cycle traverse. *Cancer Res* 32: 2720
25. Tsai CM, Gazdar AF, Venzon DJ, Steinberg SM, Dedrick RL, Mulshine JL, Kramer BS (1989) Lack of *in vitro* synergy between etoposide and *cis*-diamminedichloroplatinum(II). *Cancer Res* 49: 2390
26. Utsugi T, Aoyagi K, Furune Y, Sano M, Wierzba K, Okazaki S, Asano T, Yamada Y (1996) Antitumor activity of TAS-103, a novel topoisomerase I and II inhibitor. *Proc Am Assoc Cancer Res* 37: 427
27. Utsugi T, Aoyagi K, Furune Y, Sano M, Wierzba K, Okazaki S, Asano T, Yamada Y (1997) Antitumor activity of TAS-103, a novel topoisomerase I and II inhibitor, against orthotopically implanted human cancers. *Proc Am Assoc Cancer Res* 38: 305